Vibrations of Polar Orthotropic Laminated Shallow Spherical Shells by Godunov Method

G. Krizhevsky* and Y. Stavsky†
Technion—Israel Institute of Technology, Haifa, Israel

Introduction

THE problem of free vibrations of spherical shells has attracted great interest of investigators because of important applications of such structures in aerospace and mechanical engineering.

The classical eighth-order theory and analytical solution of the transverse vibrations of shallow isotropic spherical shell have been given by Johnson and Reissner[1] and further for the coupled longitudinal and transverse vibrations was given by Kalnins.[2] A 10th-order free vibration theory for moderately thick shallow spherical shells has been established by Kalnins.[3] A closed-form solution was obtained by the present authors for free vibrations of transversely isotropic laminated shallow spherical shells including shear deformation.[5] Generally, it is difficult (or impossible) to solve analytically dynamic problems for anisotropic spherical shells, including those with orthotropic layers. That is why approximate or numerical methods should be used.

In the current study, variational formulation is used to derive the free vibration equations of laminated shallow spherical shells composed of polar orthotropic layers for both shear deformation (SH) and the classical-type (CL) theories. These equations are solved then by the Godunov method, and some insight into the behavior of vibrating composite spherical shells is achieved by the examples shown.

Formulation of Problem

Let us consider a laminated shallow spherical cap of radius $\tilde{R}$ composed of linearly elastic polar orthotropic layers with constant thickness, $(\tilde{r}, \theta)$ are polar coordinates in the shell platform ($\tilde{r} \in [0, a]$).

The displacement distribution through the shell thickness is assumed as follows:

$$\{\tilde{u}_r, \tilde{u}_\theta, \tilde{w}\} = \{\tilde{u}_r^0, \tilde{u}_\theta^0, \tilde{w}^0\} + \{\tilde{z}\psi_1, \tilde{z}\psi_2, 0\} \tag{1}$$

where ψ_1 and ψ_2 are independent rotations of normals for SH theory, and

$$\{\psi_1, \psi_2\} = -\left\{\frac{\partial w}{\partial r}, \frac{\partial w}{r\partial\theta}\right\} \tag{2}$$

for the CL case, where $(z, r, u_r, u_\theta, w, R) = (\tilde{z}, \tilde{r}, \tilde{u}_r^0, \tilde{u}_\theta^0, \tilde{w}, \tilde{R})/a$.

The following hypotheses are assumed: thinness ($h/R \ll 1$, h is shell thickness), shallowness (following Reissner[4] it is assumed here that a shell is shallow if the condition is satisfied $\Theta \simeq \frac{1}{R} \leq \frac{1}{3}$, Θ is the half-angle of shell openness), the transverse normal stress σ_z is assumed to be zero.

Applying Hamilton's principle to the three-dimensional functional of full energy of the shell, after variation procedure and omission of the term $\exp(ipt)$, one obtains the free vibration equations in dimensionless form:

$$L_{ij}U_j = 0 \tag{3}$$

where $i, j = 1, 2, \ldots, 5$, for SH theory, and $i, j = 1, 2, 3$ for CL theory. Summing on j is supposed here.

Denoting:

$$U = \{U_1, U_2, U_3, U_4, U_5\} = \{u_r, u_\theta, w, \psi_1, \psi_2\} \tag{4}$$

operators L_{ij} and L_{ij}^* are for SH and CL theories, respectively:

$$L_{11} \equiv L_{11}^* \equiv r\frac{\partial^2}{\partial r^2} + \frac{\partial}{\partial r} - \frac{\gamma_2}{r} + \frac{\gamma_5}{r}\frac{\partial^2}{\partial\theta^2} + k_u r$$

$$L_{12} \equiv L_{12}^* \equiv \left[(\gamma_3 + \gamma_5)\frac{\partial}{\partial r} - \frac{\gamma_2 + \gamma_5}{r}\right]\frac{\partial}{\partial\theta}$$

$$L_{13} \equiv \frac{1}{R}\left[\gamma_2 - 1 - (1 + \gamma_3)r\frac{\partial}{\partial r}\right]$$

$$L_{14} \equiv \xi_1\left(r\frac{\partial^2}{\partial r^2} + \frac{\partial}{\partial r}\right) - \frac{\xi_2}{r} + \frac{\xi_5}{r}\frac{\partial^2}{\partial\theta^2} + k_{\psi 1} r$$

$$L_{15} \equiv \left[(\xi_3 + \xi_5)\frac{\partial}{\partial r} - \frac{\xi_2 + \xi_5}{r}\right]\frac{\partial}{\partial\theta}$$

$$L_{21} \equiv L_{21}^* \equiv \left[(\gamma_3 + \gamma_5)\frac{\partial}{\partial r} + \frac{\gamma_2 + \gamma_5}{r}\right]\frac{\partial}{\partial\theta}$$

$$L_{22} \equiv L_{22}^* \equiv \gamma_5\left(r\frac{\partial^2}{\partial r^2} + \frac{\partial}{\partial r} - \frac{1}{r}\right) + \frac{\gamma_2}{r}\frac{\partial^2}{\partial\theta^2} + k_u r$$

$$L_{23} \equiv -\frac{\gamma_2 + \gamma_3}{R}\frac{\partial}{\partial\theta}$$

$$L_{24} \equiv \left[(\xi_3 + \xi_5)\frac{\partial}{\partial r} + \frac{\xi_2 + \xi_5}{r}\right]\frac{\partial}{\partial\theta}$$

$$L_{25} \equiv \xi_5\left(r\frac{\partial^2}{\partial r^2} + \frac{\partial}{\partial r} - \frac{1}{r}\right) + \frac{\xi_2}{r}\frac{\partial^2}{\partial\theta^2} + k_{\psi 1} r$$

$$L_{31} \equiv \frac{1}{R}\left[(\gamma_7 + \gamma_8)r\frac{\partial}{\partial r} + \gamma_8 + \gamma_9\right]$$

$$L_{32} \equiv \frac{\gamma_8 + \gamma_9}{R}\frac{\partial}{\partial\theta}$$

$$L_{33} \equiv r\frac{\partial^2}{\partial r^2} + \frac{\partial}{\partial r} + \frac{\gamma_{45}}{r}\frac{\partial^2}{\partial\theta^2} - \frac{r}{R^2}(\gamma_7 + 2\gamma_8 + \gamma_9) + k_w r$$

$$L_{34} \equiv r\frac{\partial}{\partial r} + 1 + \frac{r}{R}\left[(\xi_7 + \xi_8)\frac{\partial}{\partial r} + \frac{\xi_8 + \xi_9}{r}\right]$$

$$L_{35} \equiv \left(\gamma_{45} + \frac{\xi_8 + \xi_9}{R}\right)\frac{\partial}{\partial\theta}$$

$$L_{41} \equiv \eta_1\left(r\frac{\partial^2}{\partial r^2} + \frac{\partial}{\partial r}\right) - \frac{\eta_2}{r} + \frac{\eta_5}{r}\frac{\partial^2}{\partial\theta^2} + k_{u1} r$$

$$L_{42} \equiv \left[(\eta_3 + \eta_5)\frac{\partial}{\partial r} - \frac{\eta_2 + \eta_5}{r}\right]\frac{\partial}{\partial\theta}$$

$$L_{43} \equiv \frac{1}{R}\left[\eta_2 - \eta_1 - (\eta_1 + \eta_3)r\frac{\partial}{\partial r}\right] - \zeta_1 r\frac{\partial}{\partial r}$$

$$L_{44} \equiv r\frac{\partial^2}{\partial r^2} + \frac{\partial}{\partial r} - \frac{\gamma_1}{r} + \frac{\gamma_6}{r}\frac{\partial^2}{\partial\theta^2} - \zeta_1 r + k_\psi r$$

Received Jan. 3, 1994; presented as Paper 94-1326 at the AIAA/ASME/ASCE/AHS/ASC 35th Structures, Structural Dynamics, and Materials Conference, Hilton Head, SC, April 18–20, 1994; revision received May 20, 1994; accepted for publication May 31, 1994.

*Postdoctoral Researcher, Faculty of Aerospace Engineering.
†Swope Professor of Mechanics, Faculty of Aerospace Engineering. Member AIAA.

$$L_{45} \equiv \left[(\gamma_4+\gamma_6)\frac{\partial}{\partial r} - \frac{\gamma_1+\gamma_6}{r}\right]\frac{\partial}{\partial\theta}$$

$$L_{51} \equiv \left[(\eta_3+\eta_5)\frac{\partial}{\partial r} + \frac{\eta_2+\eta_5}{r}\right]\frac{\partial}{\partial\theta}$$

$$L_{52} \equiv \eta_5\left(r\frac{\partial^2}{\partial r^2} + \frac{\partial}{\partial r} - \frac{1}{r}\right) + \frac{\eta_2}{r}\frac{\partial^2}{\partial\theta^2} + k_{u1}r$$

$$L_{53} \equiv -\left(\frac{\eta_2+\eta_3}{R} + \zeta_2\right)\frac{\partial}{\partial\theta}$$

$$L_{54} \equiv \left[(\gamma_4+\gamma_6)\frac{\partial}{\partial r} + \frac{\gamma_1+\gamma_6}{r}\right]\frac{\partial}{\partial\theta}$$

$$L_{55} \equiv \gamma_6\left(r\frac{\partial^2}{\partial r^2} + \frac{\partial}{\partial r} - \frac{1}{r}\right) + \frac{\gamma_1}{r}\frac{\partial^2}{\partial\theta^2} - \zeta_2 r + k_\psi r \qquad (5)$$

$$L^*_{13} \equiv L_{13} - \xi_1\left(r\frac{\partial^3}{\partial r^3} + \frac{\partial^2}{\partial r^2}\right) + \left(\frac{\xi_2}{r} - k_{\psi 1}r\right)\frac{\partial}{\partial r}$$
$$+\left(\frac{\xi_3+\xi_2+2\xi_5}{r^2} - \frac{\xi_3+2\xi_5}{r}\frac{\partial}{\partial r}\right)\frac{\partial^2}{\partial\theta^2}$$

$$L^*_{23} \equiv -\left[\frac{\gamma_2+\gamma_3}{R} + (\xi_3+2\xi_5)\frac{\partial^2}{\partial r^2} + \frac{\xi_2}{r}\frac{\partial}{\partial r}\right.$$
$$\left.+\frac{\xi_2}{r^2}\frac{\partial^2}{\partial\theta^2} + k_{\psi 1}\right]\frac{\partial}{\partial\theta}$$

$$L^*_{31} \equiv \frac{1}{R}\left[(\bar\gamma_7+\bar\gamma_8)r\frac{\partial}{\partial r} + \bar\gamma_8 + \bar\gamma_9\right] + \eta_1\left(r\frac{\partial^3}{\partial r^3} + 2\frac{\partial^2}{\partial r^2}\right)$$
$$+\frac{\eta_3+2\eta_5}{r}\frac{\partial^3}{\partial r\partial\theta^2} + \frac{\eta_2}{r^2}\left(\frac{\partial^2}{\partial\theta^2} - r\frac{\partial}{\partial r} + 1\right)$$
$$+k_{u1}\left(r\frac{\partial}{\partial r} + 1\right)$$

$$L^*_{32} \equiv \left[\frac{\bar\gamma_8+\bar\gamma_9}{R} + (\eta_3+2\eta_5)\frac{\partial^2}{\partial r^2}\right.$$
$$\left.+\frac{\eta_2}{r^2}\left(\frac{\partial^2}{\partial\theta^2} - r\frac{\partial}{\partial r} + 1\right) + k_{u1}\right]\frac{\partial}{\partial\theta}$$

$$-L^*_{33} \equiv r\frac{\partial^4}{\partial r^4} + 2\frac{\partial^3}{\partial r^3} + 2(\gamma_4+2\gamma_6)\left(\frac{1}{r}\frac{\partial^2}{\partial r^2} - \frac{1}{r^2}\frac{\partial}{\partial r} + \frac{1}{r^3}\right)$$
$$\times\frac{\partial^2}{\partial\theta^2} + \gamma_1\left(\frac{1}{r^3}\frac{\partial^4}{\partial\theta^4} + \frac{2}{r^3}\frac{\partial^2}{\partial\theta^2} - \frac{1}{r}\frac{\partial^2}{\partial r^2} + \frac{1}{r^2}\frac{\partial}{\partial r}\right)$$
$$+\frac{1}{R}\left[\frac{\bar\gamma_7+2\bar\gamma_8+\bar\gamma_9}{R}r + 2(\eta_1+\eta_3)\left(r\frac{\partial^2}{\partial r^2} + \frac{\partial}{\partial r}\right)\right.$$
$$\left.+\frac{2(\eta_2+\eta_3)}{r}\frac{\partial^2}{\partial\theta^2}\right] - \lambda^2 r \qquad (6)$$

$$\gamma_1 = D_{22}/D_{11}, \quad \gamma_2 = A_{22}/A_{11}, \quad \gamma_3 = A_{12}/A_{11}$$
$$\gamma_4 = D_{12}/D_{11}, \quad \gamma_5 = A_{66}/A_{11}, \quad \gamma_6 = D_{66}/D_{11}$$
$$\gamma_7 = A_{11}/A_{55}, \quad \gamma_8 = A_{12}/A_{55}, \quad \gamma_9 = A_{22}/A_{55}$$
$$\gamma_{45} = A_{44}/A_{55}, \quad \bar\gamma_7 = A_{11}a^2/D_{11}, \quad \bar\gamma_8 = A_{12}a^2/D_{11}$$
$$\bar\gamma_9 = A_{22}a^2/D_{11}, \quad \xi_1 = B_{11}/A_{11}a, \quad \xi_2 = B_{22}/A_{11}a$$
$$\xi_3 = B_{12}/A_{11}a, \quad \xi_4 = B_{66}/A_{55}a, \quad \xi_5 = B_{66}/A_{11}a$$
$$\xi_7 = B_{11}/A_{55}a, \quad \xi_8 = B_{12}/A_{55}a, \quad \xi_9 = B_{22}/A_{55}a$$
$$\eta_1 = B_{11}a/D_{11}, \quad \eta_2 = B_{22}a/D_{11}, \quad \eta_3 = B_{12}a/D_{11}$$
$$\eta_5 = B_{66}a/D_{11}, \quad \zeta_1 = A_{55}a^2/D_{11}, \quad \zeta_2 = A_{44}a^2/D_{11}$$
$$k_u = \lambda^2/\lambda_u, \quad k_\psi = \lambda^2/\lambda_\psi, \quad k_w = \lambda^2/\zeta_1$$
$$k_{u1} = \lambda^2\lambda_{u1}, \quad k_{\psi 1} = \lambda^2\lambda_{\psi 1}, \quad \lambda_u = A_{11}a^2/D_{11}$$
$$\lambda_\psi = R_0a^2/R_2, \quad \lambda_{u1} = R_1/R_0a$$
$$\lambda_{\psi 1} = \lambda_{u1}D_{11}/A_{11}a^2, \quad \lambda^2 = R_0p^2a^4/D_{11} \qquad (7)$$

where $\{A_{ij}, B_{ij}, D_{ij}\}$ are the stiffness matrices (with the shear correction factor assumed to be $\frac{5}{6}$), $\{R_0, R_1, R_2\}$ are the inertia moments, p is the angular frequency, and t is the time variable. A distance from the external face surface of the shell to the reference surface is chosen then to satisfy the condition $B_{11} = 0$.

The boundary conditions considered are the clamped circular edge, and the requirement of regularity at the apex is replaced here by the condition of free boundary at the circumference of a small radius δ near the apex.

Note that, for the limiting case of isotropic shell, Eqs. (5) and (6) are reduced into well-known equations given in Refs. 2 and 3.

Solution Method

The separable solutions of Eqs. (5) and (6) are presented as

$$\{u_r, w, \psi_1\} = \{u, W, \Psi_1\}\cos n\theta$$
$$\{u_\theta, \psi_2\} = \{v, \Psi_2\}\sin n\theta \qquad (8)$$

Taking into account Eq. (8), Eqs. (5) and (6) are represented in following matrix form:

$$\{Y(r)\}_{,r} = [S]\{Y(r)\}^T, \qquad \{y(r)\} = [T]\{y(r)\}^T \qquad (9)$$

along with the boundary conditions

$$[B^L]\{Y(1)\} = 0, \qquad [B^R]\{Y(\delta)\} = 0$$
$$[C^L]\{y(1)\} = 0, \qquad [C^R]\{y(\delta)\} = 0 \qquad (10)$$

where

$$\{Y\} = \{u, u', v, v', W, W', \Psi_1, \Psi_1', \Psi_2, \Psi_2'\}$$
$$\{y\} = \{u, u', v, v', W, W', W'', W'''\}$$

The terms $[S]$, $[T]$, $[B^L]$, $[B^R]$, $[C^L]$, and $[C^R]$ are numerical matrices.

According to the Godunov method,[7] the solutions of problems (8–9) are written as follows:

For SH:

$$\{Y(r)\} = \sum_{k=1}^{5} c_k\{Y(r)\}_k$$

For CL:

$$\{y(r)\} = \sum_{k=1}^{4} c_k^*\{y(r)\}_k \qquad (11)$$

where c_k and c_k^* are unknown constants, the functions $\{Y(r)\}_k$ and $\{y(r)\}_k$ satisfy the boundary conditions (8) at the left edge ($r = 1$), and initial vector sets $\{Y(1)\}_k$ and $\{y(1)\}_k$ are chosen to be linearly independent. Then the boundary conditions (9) at the right edge yield the eigenvalue equation. Functions $\{Y(r)\}_k$ and $\{y(r)\}_k$ are produced numerically by any algorithm of the initial value problem solution. Simultaneous integration of 50 for CL-case and 32 for SH-case ordinary differential equations by the Runge–Kutta–Gill method is executed here. To keep the numerical stability of computations for a wide range of system parameters, the Gram–Schmidt orthogonalization of vectors $\{Y(r_i)\}_k$ and $\{y(r_i)\}_k$ is employed after each step of the integration.

Numerical Results and Discussion

A three-layer spherical shell made of the high-strength graphite/epoxy (HSG) material with the properties $E_2/E_1 = \frac{1}{12}$, $G_{ij}/E_1 = \frac{2}{45}$, $\nu_1 = 0.27$ (E_i and G_{ij} are Young and shear moduli and ν_i is Poisson's ratio) is tried in parametric studies. The fiber orientations of the layers are specified as $\varphi = 0$ deg if the maximum Young's modulus E_1 is in meridional direction and $\varphi = 90$ deg for the circumferencially reinforced layer. The following notations are introduced in this part: $f = h/a$ and $\Omega = pa^2h\sqrt{12(1-\nu_1\nu_2)\rho/E_1}$. The thickness of the inner layer is taken to be equal to 0.2 of the shell thickness ($h_2/h = 0.2$). The radius of the inner circumference for the spherical shells is set at $\delta = 0.01$, and h_1 is the thickness of upper layer.

The comparison of results obtained by the current method with known ones[2,5,6] has shown that maximum relative difference is less than 1.5% for both CL and SH theories.

The dependences of the first two dimensionless natural frequencies Ω of a polar orthotropic three-layer shallow spherical cap on the inner layer location (defined by the h_1/h ratio) are shown in Fig. 1a (0/90/0 lamination) and Fig. 1b (90/0/90 lamination). It is shown that the 0/90/0 lamination yields a higher value of natural frequencies than the 90/0/90 lamination. For the axisymmetric eigenmode ($n = 0$), the 0/90/0 shell with small h_1 has the highest natural frequency (Fig. 1a), whereas for the 90/0/90 lamination the highest value of the natural frequency is reached with small h_3 (Fig. 1b) (h_3 is the thickness of the lower layer). This is explained by the larger dynamic stiffness of the 0-deg layer for the axisymmetric eigenmode.

The dependences of the first two dimensionless natural frequencies Ω of symmetrically laminated three-layer shallow spherical shells on the half-angle of openness Θ are shown in Figs. 2a and 2b, respectively. It can be seen that for both shell types the frequency associated with the axisymmetric mode shape ($n = 0$) is more sensitive to the Θ change. That is why the tendency to the rearrangement in the order of eigenmodes is observed with increased Θ; that is, after a certain value of Θ, the lowest frequency is associated with the asymmetric mode shape (see, for example, graphs 3 and 6 in Fig. 2a).

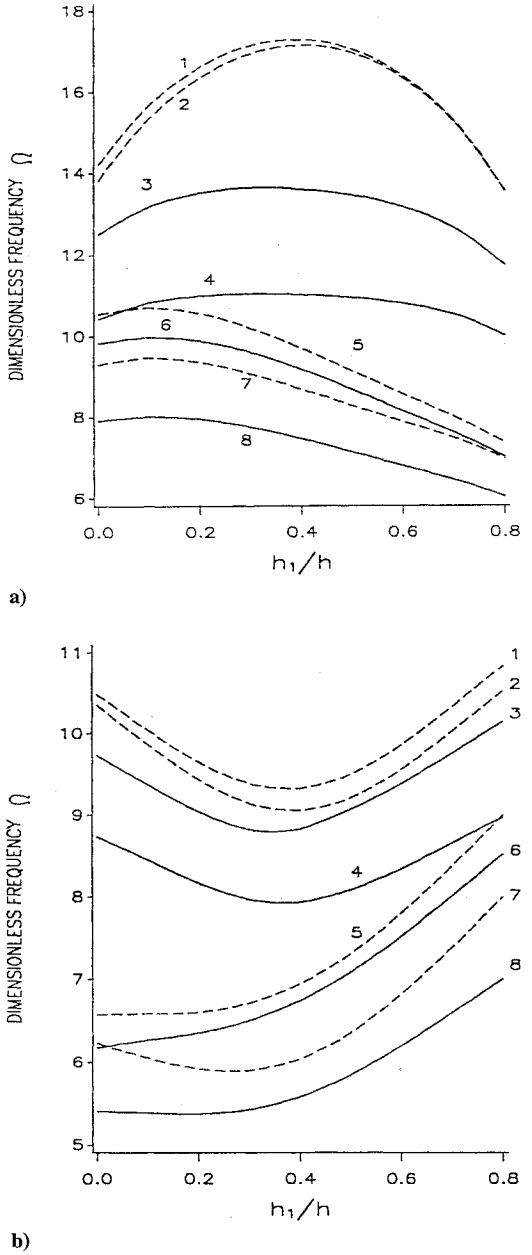

Fig. 1 Spherical cap, $\Theta = 10$ deg; curves with $n = 1$: 1 and 3—$f = 0.1$, 2 and 4—$f = 0.15$; curves with $n = 0$: 5 and 6—$f = 0.1$, 7 and 8—$f = 0.15$; solid lines are for the SH case and dashed lines are for the CL case: a) 0/90/0 and b) 90/0/90.

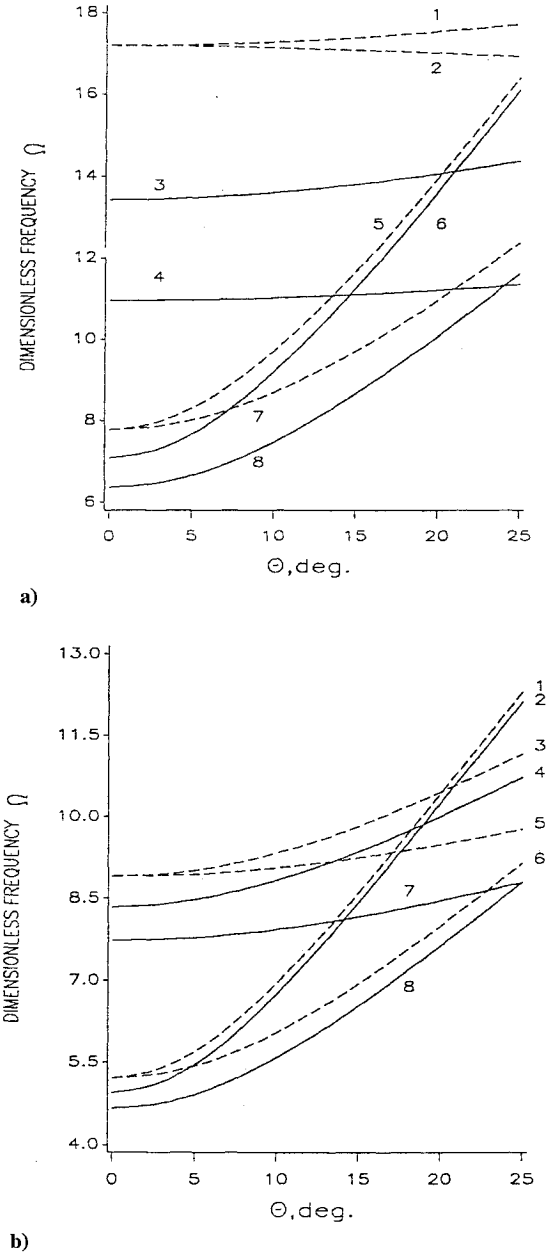

Fig. 2 Spherical cap, $h_1/h = 0.4$; curves with $n = 1$: 1 and 3—$f = 0.1$, 2 and 4—$f = 0.15$; curves with $n = 0$: 5 and 6—$f = 0.1$, 7 and 8—$f = 0.15$; solid lines are for the SH case and dashed lines are for the CL case: a) 0/90/0 and b) 90/0/90.

The comparison of results predicted by the SH and CL theories shows that differences between them increase with the increase of relative thickness, as well as with a rise in the number of an eigenmode (Figs. 1 and 2). For example, for the 0/90/0 lamination with $h_1/h = 0.4$ and $h/a = 0.15$, the frequency ratio associated with the first vibrational mode $\Omega_{00}^{CL}/\Omega_{00}^{SH} = 1.16$, whereas for the second mode $\Omega_{01}^{CL}/\Omega_{01}^{SH} = 1.56$ (see Fig. 1a, graphs 2 and 4 and graphs 7 and 8).

The convergence of SH and CL results is observed with an increase in Θ (Figs. 2a and 2b).

Acknowledgments

The work of G. Krizhevsky was supported by the Center for Absorption in Science, Ministry of Immigrant Absorption, State of Israel, and the Swope Chair of Mechanics. The work of Y. Stavsky was supported by the Swope Chair of Mechanics and the Technion Fund for Promotion of Research.

References

[1]Johnson, M. W., and Reissner, E., "On Transverse Vibrations of Shallow Spherical Shells," *Quarterly of Applied Mathematics*, Vol. 15, No. 4, 1958, pp. 367–380.

[2]Kalnins, A., "Free Non-Symmetric Vibrations of Shallow Spherical Shells," *Proceedings of 4th U.S. National Congress of Applied Mechanics*, American Society of Mechanical Engineers, New York, 1962, pp. 225–233.

[3]Kalnins, A., "On Vibrations of Shallow Spherical Shells," *Journal of the Acoustical Society of America*, Vol. 33, No. 6, 1961, pp. 1102–1107.

[4]Reissner, E., "Symmetric Bending of Shells of Revolution," *Journal of Mathematics and Mechanics*, Vol. 7, No. 2, 1958, pp. 121–140.

[5]Krizhevsky, G., and Stavsky, Y., "Mindlin-Type Vibration Theory for Laminated Transversally Isotropic Shallow Spherical Shells," *Proceedings of 5th International Conference of Recent Advances in Structural Dynamics* (Southampton, UK), 1994 (to be published).

[6]Soamidas, V., and Ganesan, N., "Asymmetric Vibrations of Layered Shells of Revolution," *Journal of Sound and Vibrations*, Vol. 147, No. 1, 1991, pp. 39–56.

[7]Godunov, S. K., "On the Numerical Solution of Boundary Value Problems for Systems of Linear Ordinary Differential Equations," *Uspekhi Mathematicheskikh Nauk (Advances in Mathematical Sciences)*, Vol. 16, No. 3, 1961, pp. 171–174.

Genetic-Algorithm-Based Procedure for Pretest Analysis

Claudio G. Franchi* and Daniele Gallieni*
Politecnico di Milano, Milan 20133, Italy

Nomenclature

$\mathcal{A}$	= $2n_M \times 2n_M$ state matrix
C	= damping $n \times n$ matrix of the system
$\mathcal{F}$	= vector of the $2n_M$ inputs
F	= vector of the n external forces
K	= stiffness $n \times n$ matrix of the system
M	= mass $n \times n$ matrix of the system
q	= vector of the n degrees of freedom
S	= $m \times 2n$ matrix formed by zeros and ones
svd($\mathcal{O}$)	= singular values of the $\mathcal{O}$ matrix
x	= vector of the $2n_M$ states
Δ_j	= integer parameter that assumes the values 0 or 1
ξ_i	= adimensional damping coefficients
ω_i	= natural frequencies of the system
$(\dot{})$	= time derivative

Received Jan. 27, 1994; revision received Aug. 23, 1994; accepted for publication Aug. 23, 1994.

*Department of Aerospace Engineering.

I. Introduction

THE optimization of the test setup in experimental modal analysis, the so called pretest analysis, is important to allow the execution of vibration tests on large structures. To reduce measurement time and cost, the test has to be performed using the least number of sensors and shakers that will identify the structural modes in the measured frequency range.[1] This paper issues the optimal layout of sensors for experimental modal testing as a testbed for using genetic-algorithm (GA)[2]-based procedures in the solution of sensors and actuators optimal placement for adaptive structures design.[3–5]

In the pretest phase, only the results of numerical modal analysis are available and used to look for the optimal sensors layout. The sensors position defines the subset of measured degrees of freedom (DOF) in the set of finite element mesh DOFs. Pretest analysis looks for the best choice of the elements of this subset by assembling a reduced experimental model defined by measured DOFs only. In many actual problems the number of DOFs of the finite elements model n is quite large, although the experimental measurements can be performed just at few points. Thus, calling m the number of measured points, $m \ll n$. The problem of finding the best subset of m measurement points in a n sized mesh belongs to the family of combinatorial optimization which requires the simple combinations of n elements in a class of m.

For real problems the number of independent solutions is very large, and enumerative methods become computationally useless. On the other hand, the discrete nature of this problem suggests the avoidance of the use of analytical optimization methods both due to the lack of gradient informations and robustness in direction finding procedures. This kind of problem presents many local optima; and gradient information allows local peaks to be reached leading to solutions depending on the starting conditions. A more feasible approach is represented by a combinatorial method, which treats the coordinate of a grid node as a two-state variable. The latter can be switched on, if chosen to a measure point, or switched off, when inactive. By following this discrete formulation, several heuristic methods have been proposed[6,7] although most of them do not fit completely in the combinatorial nature of the present task. In fact, they cannot treat the whole set of measured DOFs as a single optimization variable but treat each of its elements one at a time. The drawback of finding local optima is overcome by using either simulated annealing or other stochastic algorithms. These methods allow, at least during the initial phase of the optimization, movement toward nonimproving solutions. Moreover, the methods deal with a set of points in solution space, thus avoiding that the solution to be dependent on initial guess.[8]

Many features of the GA meet the discussed requirements and thus, its suitability is suggested for solving these kind of problems.[9] The features are summarized in the following points:

1) GA allows the direct treatment of the set of measured DOFs as a single optimization variable, instead of assigning one variable to any measured DOF. Moreover, a discrete problem can be implemented by considering the integer numbers that represent the DOFs in the finite element model as optimization variables.

2) Like other stochastic methods, GA evaluates at any iteration a number of different solutions equal to the number of individuals of the population. This fact guarantees that the solution will converge to a sufficiently general optimum, regardless of the starting guess. The optimization procedure is based only on the evaluation of the objective function, without any need of gradient information.

3) GA shows all of the generality typical of simulated annealing and other stochastic methods. Its strength comes from the use, beside these techniques, of evolutionary criteria in selection. This fact guarantees a fruitful equilibrium in selecting good solutions among the available ones and exploitation of new directions in solutions space by generating new genetic material from well performing old individuals.

4) The computational effort does not directly depend on the combinatorial order of the problem but is related to the size of the popula-